Available online at www.sciencedirect.com
SCIENCE DIRECT®
C. R. Mecanique 334 (2006) 158–163
COMPTES RENDUS MECANIQUE
http://france.elsevier.com/direct/CRAS2B/

Rainwater rivulets on a cable subject to wind

Cécile Lemaitre [a], Md. Mahmud Alam [b], Pascal Hémon [a], Emmanuel de Langre [a,*], Yu Zhou [b]

[a] *Département de Mécanique, LadHyX, École polytechnique, 91128 Palaiseau, France*
[b] *Department of Mechanical Engineering, The Hong Kong Polytechnic University, Hung Hom, Kowloon, Hong Kong*

Received 18 December 2005; accepted 19 January 2006

Available online 28 February 2006

Presented by Pierre Perrier

Abstract

Rainwater rivulets appear on inclined cables of cable-stayed bridges when wind and rain occur simultaneously. In a restricted range of parameters this is known to cause vibrations of high amplitudes on the cable. The mechanism underlying this effect is still under debate but the role of rainwater rivulets is certain. We use a standard lubrication model to analyse the dynamics of a water film on a cylinder under the effect of gravity and wind load. A simple criterion is then proposed for the appearance and position of rivulets, where the Froude number is the control parameter. Experiments with several geometries of cylinder covered with water in a wind tunnel show the evolution of the rivulets with the Froude number. Comparison of the prediction by the model with these experimental data shows that the main mechanism of rivulet formation and positioning is captured. ***To cite this article: C. Lemaitre et al., C. R. Mecanique 334 (2006).***

Résumé

Filets d'eau de pluie sur un câble soumis au vent. Des filets d'eau de pluie apparaissent sur les haubans inclinés de ponts lorsque le vent et la pluie sont présents simultanément. Pour certaines conditions ceci peut causer des vibrations de grandes amplitudes de ces haubans. Le mécanisme précis à l'origine de cet effet est encore l'objet de débat, mais le rôle de ces filets est certain. Nous utilisons un modèle de film mince pour analyser la dynamique d'un film d'eau sur un cylindre, sous l'action de la gravité et du chargement dû au vent. Un critère simple est proposé pour prédire l'apparition et la position des filets, dans lequel le nombre de Froude est le paramètre de contrôle. Des expériences avec différents cylindres couverts d'eau et placés dans une soufflerie montrent l'évolution de ces filets avec le nombre de Froude. La comparaison entre les prédictions du modèle et les données expérimentales permet d'affirmer que le mécanisme principal de création et de positionnement des filets est décrit par ce modèle. ***Pour citer cet article : C. Lemaitre et al., C. R. Mecanique 334 (2006).***

Keywords: Vibrations; Rain; Wind; Rivulet; Cylinder

Mots-clés : Vibrations ; Vent ; Pluie ; Filet ; Cylindre

* Corresponding author.
E-mail address: delangre@ladhyx.polytechnique.fr (E. de Langre).

1631-0721/$ – see front matter
doi:10.1016/j.crme.2006.01.005

Version française abrégée

On considère le cas simplifié d'un câble incliné dans le sens du vent, Fig. 1(a) et on étudie l'évolution d'un film liquide sur la surface du cylindre, Fig. 1(b). A l'aide d'un modèle de film mince combinant le modèle de Reisfeld [8] et d'Oron [9] on déduit l'équation d'évolution de l'épaisseur, Éq. (3), en fonction des efforts de gravité, de tension superficielle (nombre de Bond) et ceux dûs au vent (nombre de Froude). Le modèle simple proposé en Section 3 est fondé sur l'hypothèse que les filets vont apparaître, sur un film uniforme, au lieu où la croissance du film est maximale. Cette croissance, Éq. (4), peut être simplement analysée en fonction du nombre de Froude, Fig. 2. On montre alors que pour de faibles vitesses de vent un filet se forme au vent du cylindre, et qu'il se divise en deux filets qui vont se fixer près des points de séparation au dessus d'un nombre de Froude critique, Éq. (5). Dans la Section 4 on présente les résultats d'une série d'essais en soufflerie avec un cylindre couvert d'un film d'eau ruisselant, pour différents diamètres de cylindre et angles d'inclinaison, Fig. 3(a). La position des filets est suivie par une technique optique. La comparaison entre les prédictions du modèle et les points expérimentaux, Fig. 3(b), montre que la transition entre les deux régimes est bien observée dans l'expérience et prédite par les calculs. L'utilisation de valeurs de coefficients de pression et de friction correspondant à un écoulement subcritique et supercritique permet d'encadrer les résultats experimentaux.

1. Introduction

Cables of cable-stayed bridges can experience strong vibrations under the combined effect of rain and wind [1]. This is commonly referred to as Rain Wind Induced Vibration (RWIV) and has been the subject of significant work in recent years, because of its importance in the design of long bridges [2–7]. In this phenomenon the dynamics of the vibrating cable and of the oscillating wind wake are coupled through the dynamics of rivulets, by a mechanism that is still under debate. These rivulets are formed from the film of rainwater flowing along inclined cables. It is common knowledge in this field [5,7], that their position on the cable seems close to the separation point of the external wind flow, and that a rivulet appears on the upper side of the cable only if the wind velocity is sufficiently high [1]. The existence of such rivulets is known to be essential to the occurrence of RWIV [2,5].

We investigate the condition for the appearance of rivulets and the relation between their position and the physical parameters of the system such as wind velocity, surface tension, viscosity of water, thickness of the water film, cable diameter and inclination. In Section 2 the equation governing the dynamics of a thin film of liquid on a cylinder subjected to wind is derived. This allows us, in Section 3, to propose a simple criterion to estimate the position of the rivulets. The predictions based on the criterion are then compared with new experimental data in Section 4.

2. Dynamics of a film under wind load

To analyse the formation of rivulets we consider a thin liquid film on a cylinder, flowing along the cylinder axis. Its shape is influenced by the effect of gravity, surface tension and wind load. A simplified configuration is considered, where the cylinder declines in the direction of wind. Typical orders of magnitudes of the parameters in our case are a ratio of film thickness to the cylinder radius of 10^{-2}, a Reynolds number for the wind flow of about 10^4 while the Reynolds number for the flow of rainwater along the cylinder is about 10^2.

In this section we derive the equation satisfied by the local thickness of the film, noted $h(\theta, t)$, in a given cross-section of the cylinder, Fig. 1(b). The forces acting on the film in that plane are gravity, of magnitude $g \sin\alpha$ where α is the inclination of the cable, and wind load, due to an upstream uniform velocity noted v_∞, which reduces to $v = v_\infty \cos\alpha$ in the cross-section plane. The resulting wind load is defined by the local pressure $p(\theta)$ and the local friction shear force $\tau(\theta)$, acting respectively on the instantaneous normal and tangent to the surface of the liquid film, Fig. 1(b).

We follow an approach similar to that used in [8]. These authors derived the equation of motion of a liquid film on a cylinder under the action of gravity and surface tension. The addition of pressure and friction forces due to the air flow follows the approach used in [9] for the case of a film on a flat surface. The derivation is done in the framework of lubrication where both the relative film thickness h/R and its gradient $h_{,\theta}/R$ are small. We also neglect here the effect of the water velocity in the direction of the cylinder axis, normal to the plane of Fig. 1(b). The dimensionless quantities that are relevant to that case are, following [8]

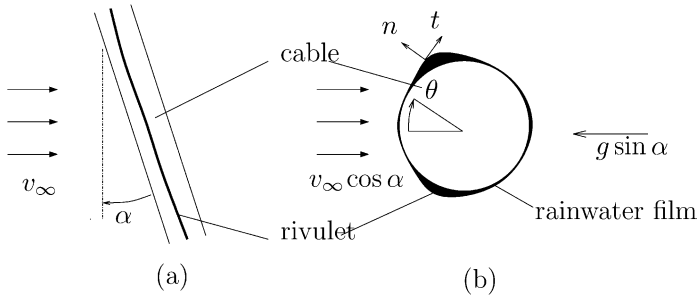

Fig. 1. Rivulet of rainwater flowing along an inclined cable subjected to wind: (a) side view; (b) cross-section.

Fig. 1. Filet d'eau de pluie s'écoulant le long d'un câble incliné soumis au vent : (a) vue de côté ; (b) coupe.

$$G = \frac{gh_0^3}{3\nu^2}, \qquad S = \frac{\gamma h_0^4}{3\rho_L \nu^2 R^3}, \qquad \mathcal{M} = \frac{\rho}{\rho_L}, \qquad \mathcal{P} = \frac{v^2 h_0^3}{6\nu^2 R}$$
$$C_P = \frac{2p}{\rho v^2}, \qquad C_F = \frac{2\tau}{\rho v^2}, \qquad T = \frac{\nu}{Rh_0}t \tag{1}$$

and $\varepsilon = h_0/R$, $H = h/h_0$, where h_0 is a reference film thickness, γ is the surface tension, ν is the viscosity of the liquid, ρ and ρ_L are the densities of air and water, C_P and C_F being the pressure and friction coefficient. Keeping only the terms at the leading order in ε in a derivation identical to that of [8] leads here to the equation governing the dynamics of the film [10,11]

$$H_{,T} = G\sin\alpha\left(H^3\sin\theta\right)_{,\theta} - S\left[H^3(H_{,\theta} + H_{,\theta\theta\theta})\right]_{,\theta} + \mathcal{M}\mathcal{P}\left[H^3 C_{P,\theta} - H^2\frac{3}{2\varepsilon}C_F\right]_{,\theta} \tag{2}$$

where $(\,,\,)$ stands for differentiation. It should be noted here that the friction coefficient C_F being of the order of 10^{-2}, which is similar to that of ε in practice, the last term C_F/ε needs to be kept at this order, as in [9]. When $\mathcal{P}$ is set to zero (no wind), Eq. (2) is identical to that of [8]. Conversely, when G is set to zero and when C_P and C_F do not depend on θ, in the limit of large cable radius the equation of [9] for the dynamics of a plane film subjected to air flow is obtained from Eq. (2).

Another dimensionless form, of more practical use, can be defined by rescaling the time variable by gravity, $\tau = GT\sin\alpha$, so that Eq. (2) now reads

$$H_{,\tau} = \left(H^3\sin\theta\right)_{,\theta} - Bo^{-1}\left[H^3(H_{,\theta} + H_{,\theta\theta\theta})\right]_{,\theta} + \frac{1}{2}\mathcal{M}F_R^2\left[H^3 C_{P,\theta} - H^2\frac{3}{2\varepsilon}C_F\right]_{,\theta} \tag{3}$$

where the Bond number $Bo = G/S = \rho_L g R^3\sin\alpha/(\gamma h_0)$ and the Froude number $F_R^2 = \mathcal{P}/G = v^2/(gR\sin\alpha)$ are now used. In order to compare the effect of gravity, surface tension and wind load on the dynamics of the film, the following order of magnitude of the parameters can be used: $v^2 = 10\ \mathrm{m}^2/\mathrm{s}^2$, $\sin\alpha = 0.1$, $R = 10^{-2}$ m, $\varepsilon = 10^{-2}$, $\gamma = 10^{-1}$ N/m, $\rho = 1\ \mathrm{kg/m}^3$, $\mathcal{M} = 10^{-3}$. This results in $Bo^{-1} = 10^{-2}$ and $\mathcal{M}F_R^2 = 1$, showing that all terms in Eq. (3) play a role, but that the effect of surface tension is not dominant.

3. Position of rivulets

If a uniform film on the cylinder is subjected to the effect of gravity and of wind load its evolution is governed by Eq. (3). To estimate the location of rivulets that will result from this evolution we may simply compare the local growth rate of the film thickness, as defined by the right-hand side term of Eq. (3), on all points around the cylinder. This growth rate, on a film of uniform thickness $H = 1$ reduces to

$$r(\theta) = \cos\theta + \frac{1}{2}\mathcal{M}F_R^2\left[C_{P,\theta\theta} - \frac{3}{2\varepsilon}C_{F,\theta}\right] \tag{4}$$

We now assume that a rivulet will grow and eventually stabilize through non-linear effects at the location, noted θ_R, where the local growth rate of a uniform film, $r(\theta)$, is maximum.

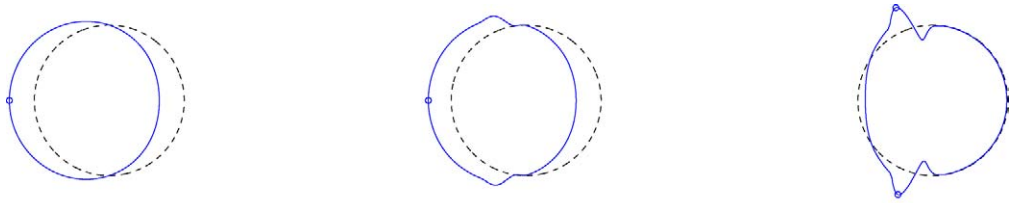

Fig. 2. Comparative local growth rate on a uniform thin film around a cylinder under the combined action of gravity and wind load. (—) growth rate, shown as a polar function with arbitrary scale. (o) position of the maximum of growth rate, θ_R, where the rivulet appears. (a) $\mathcal{M}F_R^2 = 0$: rivulet resulting from gravity, growing at $\theta_R = 0$. (b) $\mathcal{M}F_R^2 = 0.01$, (c) $\mathcal{M}F_R^2 = 10$: rivulet resulting from wind load, growing at $\theta_R/\pi = 0.38$.

Fig. 2. Taux de croissance relatif sur un film uniforme autour d'un cylindre sous l'action simultanée de la gravité et du chargement du vent (—) taux de croissance vu comme une fonction polaire et d'amplitude arbitraire (o) position du taux de croissance maximum, θ_R, où le filet va apparaître. (a) $\mathcal{M}F_R^2 = 0$: filet dû à la gravité, croissant à $\theta_R = 0$. (b) $\mathcal{M}F_R^2 = 0{,}01$, (c) $\mathcal{M}F_R^2 = 10$: filet dû au vent, croissant à $\theta_R/\pi = 0{,}38$.

Using Eq. (4) the growth rate is plotted as a function of the position around the cylinder, for several values of the Froude number, Fig. 2. As this parameter is increased the position of the maximum of the growth rate shifts from the front of the cylinder, $\theta_R = 0$, where gravity dominates for $\mathcal{M}F_R^2 \ll 1$, to an angle noted $\theta_R = \theta_R^{\max}$ for $\mathcal{M}F_R^2 \gg 1$. This shift results from the competition between the two terms of Eq. (4), the last one depending on the Froude number. Using the data of [12] for the coefficients $C_P(\theta)$ and $C_F(\theta)$, which depend on the range of Reynolds number, we have typically, $\theta_R^{\max}/\pi = 0.38$ in the subcritical range and $\theta_R^{\max}/\pi = 0.51$ in the supercritical range. This is close, though not identical, to the position of the separation point on a cylinder without film. Though the Reynolds number considered here is only 10^4 we give results for subcritical and supercritical conditions as this may apply for practical cases.

The transition between the two regimes, i.e., one rivulet at $\theta_R = 0$ or two symmetrical rivulets at $\theta_R = \theta_R^{\max}$ can be estimated by comparing the value of the growth rate $r(\theta)$ at these two points. This yields a simple critical value of the control parameter

$$\left(\mathcal{M}F_R^2\right)_C = \frac{2(1-\cos\theta_R^{\max})}{C_{P,\theta\theta}(\theta_R^{\max}) - \frac{3}{2\varepsilon}C_{F,\theta}(\theta_R^{\max})} \tag{5}$$

This allows us to predict a transition at $(\mathcal{M}F_R^2)_C = 0.05$ and $(\mathcal{M}F_R^2)_C = 0.1$ for subcritical or supercritical values of the pressure and friction coefficients, respectively.

4. Comparison with experiments

A new set of experiments has been performed at the Mechanical Engineering Department of Hong Kong Polytechnic University. The set-up is presented on Fig. 1(a). An inclined cylinder in a wind tunnel is covered with a thin film of colored water (milk) that is fed at the top by a funnel. The position of the rivulets is measured optically. The Froude number, which was found in the model above to be the main control parameter, is varied by changing the flow velocity v_∞ from 0 to 15 m/s, the inclination of the cylinder α from 2.5 to 35 degrees, or the radius of the cylinder R from 7.5 to 11 mm. The flow rate is such that the film thickness on the vertical cylinder without wind is $h_0 \simeq 10^{-4}$ m, so that the ratio is $\varepsilon \simeq 10^{-2}$.

Fig. 3(b) shows the evolution of the position of the rivulet with the Froude number. For a given radius and inclination angle, when the flow velocity is increased it is observed that the windward rivulet, originally at $\theta = 0$, splits in two rivulets that migrate to a position that does not change for higher Froude numbers, about $\theta_R/\pi = 0.44$. This transition occurs between $\mathcal{M}F_R^2 = 0.1$ and $\mathcal{M}F_R^2 = 1$. The results of experiments with different diameters and inclination angles follow the same trend when the Froude number is used as the control parameter, Fig. 3(b).

The prediction resulting from the model based in the maximum of the growth rate is shown on the same graph. Two cases are shown, using subcritical or supercritical values of the pressure and friction coefficients. In the experiments the Reynolds number is such that only subcritical conditions would be expected on a dry cylinder. Still, because of the presence of a rivulet near the separation point a transition may occur, so that supercritical data should also be considered [13]. The experimental positions of the rivulets for high velocities fall between the values given by the

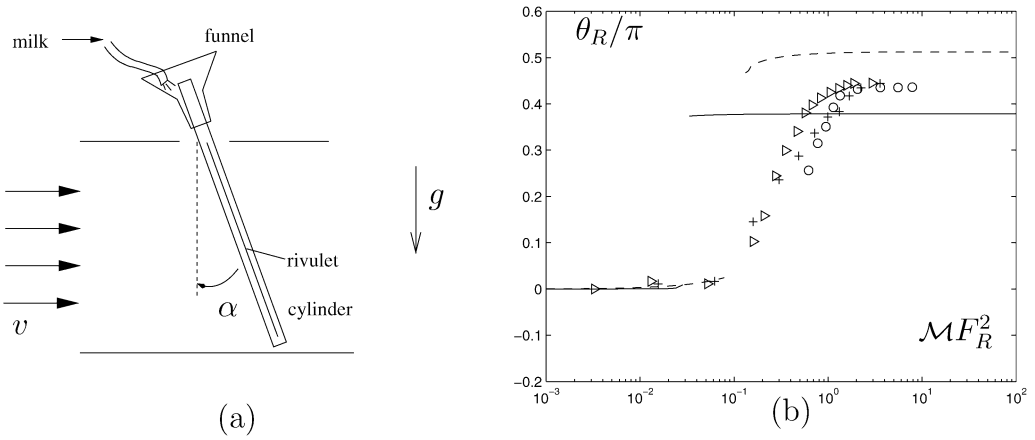

Fig. 3. Position of the rivulets on a cylinder inclined in the leeward direction. (a) Experimental set-up. (b) Experimental data: (o), $\alpha = 2.5$ deg, $R = 7.5$ mm; (▷), $\alpha = 10$ deg, $R = 11$ mm; (+), $\alpha = 35$ deg, $R = 11$ mm. A symmetrical rivulet exists at $-\theta_R$ but is not shown here for clarity. Proposed model based on the maximum of the growth rate of a uniform film, Eq. (4): (—) prediction using subcritical data on the pressure and friction coefficients; (- -) prediction using supercritical data.

Fig. 3. Position des filets sur un cylindre incliné vers l'aval. (a) Montage expérimental (b) Resultats expérimentaux (o), $\alpha = 2{,}5$ deg, $R = 7{,}5$ mm ; (▷), $\alpha = 10$ deg, $R = 11$ mm ; (+), $\alpha = 35$ deg, $R = 11$ mm. Un filet symétrique existe à $-\theta_R$ mais n'est pas montré dans un souci de clarté. Modèle proposé fondé sur le maximum de taux de croissance sur un film uniforme, Éq. (4) : (—) prédiction avec des données de coefficients de pression et de pression souscritiques (- -) prédiction avec des données dans le domaine supercritique.

model. The transition predicted in the model, using Eq. (5), is observed for lower values of the Froude number than in the experiment.

By comparing the model proposed here with experimental data it is shown that the appearance of rivulets can be explained by a balance between gravity and wind load, the Froude number being the relevant parameter to scale these effects. The equilibrium shape of a rivulet may only be computed by considering the full non-linear effect in the film equation (3) and in contact angles at the boundaries of the film if it dries in some regions of the cylinder surface. Yet the overall position seems to depend more on the variation of the external load than on local non-linear effects. In terms of practical applications to cables in cable-stayed bridges the present formulations can easily be extended to account for a cable inclination that is not the direction of wind. Moreover, for higher cable diameter, typically $R = 0.1$ m on bridges the Reynolds number is such that supercritical data on wind load should be used.

Acknowledgements

The authors acknowledge the financial support of the France-Hong Kong PROCORE joint research program 07708UE on Rain–Wind Induced Vibrations of cables.

References

[1] Y. Hikami, N. Shiraishi, Rain–wind induced vibrations of cables in cable-stayed bridges, Journal of Wind Engineering and Industrial Aerodynamics 29 (1988) 409–418.
[2] H. Yamaguchi, Analytical study on growth mechanism of rain vibration of cables, Journal of Wind Engineering and Industrial Aerodynamics 33 (1990) 73–80.
[3] M. Matsumoto, N. Shiraishi, M. Kitawaza, C. Knisely, H. Shirato, Y. Kim, M. Sujii, Aerodynamic behaviour of inclined circular cylinders cable aerodynamics, Journal of Wind Engineering and Industrial Aerodynamics 33 (1990) 63–72.
[4] O. Flamand, Rain–wind induced vibration of cables, Journal of Wind Engineering and Industrial Aerodynamics 57 (1995) 353–362.
[5] A. Bosdogianni, D. Olivari, Wind- and rain-induced oscillations of cables of stayed bridges, Journal of Wind Engineering and Industrial Aerodynamics 64 (1996) 171–185.
[6] N. Cosentino, O. Flamand, C. Ceccoli, Rain–wind induced vibration of inclined stay cables. Part I: Experimental investigation and physical explanation, Wind and Structures 6 (2003) 471–484.
[7] Z.J. Wang, Y. Zhou, J.F. Huang, Y.L. Xu, Fluid dynamics around an inclined cylinder with running water rivulets, Journal of Fluids and Structures 21 (1) (2005) 49–64.
[8] B. Reisfeld, S.G. Bankoff, Non-isothermal flow of a liquid film on a horizontal cylinder, Journal of Fluid Mechanics 236 (1992) 167–196.

[9] A. Oron, S.H. Davis, S.G. Bankoff, Long-scale evolution of thin liquid films, Reviews of Modern Physics 69 (3) (1997) 931–980.
[10] C. Lemaitre, P. Hémon, E. de Langre, Thin film around a cable subject to wind, in: 4th European African Conference on Wind Engineering, Prague, Czech Republic, July 2005, pp. 202–203.
[11] C. Lemaitre, E. de Langre, P. Hémon, Évolution d'un film d'eau autour d'un hauban de pont sous l'action du vent, in: Congrès Français de Mécanique, August 2005, paper 810.
[12] E. Achenbach, Distribution of local pressure and skin friction around a circular cylinder in a cross-flow up to $Re = 5 \times 10^6$, Journal of Fluid Mechanics 34 (4) (1968) 625–639.
[13] E. Szechenyi, Supercritical Reynolds number simulation for two-dimensional flow over circular cylinders, Journal of Fluid Mechanics 70 (3) (1975) 529–542.